9-2018

# Early Term Effects of rhBMP-2 on Pedicle Screw Fixation in a Sheep Model: Histomorphometric and Biomechanical Analyses

Jeffrey M. Toth
*Marquette University*, jeffrey.toth@marquette.edu

Mei Wang
*Marquette University*, mei.wang@marquette.edu

Chetan Patel
*Florida Hospital Medical Group*

Akshi Arora
*Marquette University*

Original Study

# Early term effects of rhBMP-2 on pedicle screw fixation in a sheep model: histomorphometric and biomechanical analyses

**Jeffrey M. Toth[1,2], Mei Wang[1,2], Chetan K. Patel[3], Akshi Arora[2]**

[1]Department of Orthopaedic Surgery, The Medical College of Wisconsin Inc., Milwaukee, WI, USA; [2]Orthopaedic & Rehabilitation Engineering Center and Graduate Program in Dental Biomaterials, Marquette University, Milwaukee, WI, USA; [3]Spine Health Institute, Florida Hospital Medical Group, Altamonte Springs, FL, USA

*Contributions:* (I) Conception and design: CK Patel, JM Toth, M Wang; (II) Administrative support: None; (III) Provision of study materials or patients: None; (IV) Collection and assembly of data: JM Toth, M Wang, A Arora; (V) Data analysis and interpretation: All authors; (VI) Manuscript writing: All authors; (VII) Final approval of manuscript: All authors.

*Correspondence to:* Jeffrey M. Toth, PhD. Department of Orthopaedic Surgery, The Medical College of Wisconsin Inc., 9200 W. Wisconsin Ave. Box 26099, Milwaukee, WI 53226-0099, USA. Email: jtoth@mcw.edu.

**Background:** The effects of recombinant human bone morphogenetic protein-2 (rhBMP-2) on pedicle screw pullout force and its potential to improve spinal fixation have not previously been investigated. rhBMP-2 on an absorbable collagen sponge (ACS) carrier was delivered in and around cannulated and fenestrated pedicle screws in a sheep lumbar spine instability model. Two control groups (empty screw and ACS with buffer) were also evaluated. We hypothesized that rhBMP-2 could stimulate bone growth in and around the cannulated and fenestrated pedicle screws to improve early bone purchase.

**Methods:** Eight skeletally mature sheep underwent destabilizing laminectomies at L2–L3 and L4–L5 followed by stabilization with pedicle screw and rod constructs. An ACS carrier was used to deliver 0.15 mg of rhBMP-2 within and around the cannulated and fenestrated titanium pedicle screws. Biomechanics and histomorphometry were used to evaluate the early term results at 6 and 12 postoperative weeks.

**Results:** rhBMP-2 was unable to improve bony purchase of the cannulated and fenestrated pedicle screws compared to both control groups. Although rhBMP-2 groups had pullout forces that were less than both control groups, both rhBMP-2 groups had pullout force values exceeding 2,000 N, which was comparable to previously published results for unmodified pedicle screws. Significant differences in the percentages of bone in peri-screw tissues was not observed amongst the four treatment groups. Microradiography and quantitative histomorphometry showed that at 6 weeks, rhBMP-2 induced peri-screw remodeling regions containing peri-implant bone which was hypodense with respect to surrounding native trabeculae. A moderate correlation between biomechanical pullout variables and histomorphometry data was observed.

**Conclusions:** The design of the cannulated and fenestrated pedicle screw was able to facilitate new bone formation to achieve high pullout forces. However, delivery of rhBMP-2 should be carefully controlled to prevent excessive bone remodeling which could cause early screw loosening.

**Keywords:** Bone morphogenetic protein 2 (BMP-2); recombinant human BMP-2 (rhBMP-2); titanium; pedicle screws; sheep model; arthrodesis; spinal fusion; instrumented; histology; histomorphometry

Submitted Oct 12, 2017. Accepted for publication Mar 13, 2018.
doi: 10.21037/jss.2018.06.19
**View this article at:** http://dx.doi.org/10.21037/jss.2018.06.19

## Introduction

Posterior pedicle screw fixation is one of the most widely used reconstructive procedures of the spine, ranging from degenerative spondylolisthesis, deformity, tumor, to spinal fractures. It has often been used as the "gold" standard of posterior fixation studies (1-4). Failure to induce a spine fusion at the operative level(s) may cause loosening of pedicle screw fixation with attendant loss of correction or non-union. Pedicle screw fixation failure through loosening, back out, or breakage of the screws has been reported in the literature (5). Preventing screw fixation failures is especially challenging in treating patients with comorbidities such as osteoporosis. Various augmentation techniques and new screw designs have been proposed to enhance the anchoring strength of the screws either in primary or salvage procedures (6-8). Augmentation approaches include injection of polymethyl methacrylate (PMMA) bone cement (9-12) or enhanced with calcium sulfate cement (13), calcium phosphates and cement (14-16), or other materials (17). Hydroxyapatite-coated screws have also been shown to improve the bone-to-implant contact in osteopenic bone and increase the pullout strength (18-21).

Recombinant human bone morphogenetic protein-2 (rhBMP-2) delivered on an absorbable collagen sponge (ACS) is a well-studied osteoinductive protein that promotes new bone formation. Application of rhBMP-2 on a carrier induces local bone formation and has been used as a bone graft substitute in the spine (22-27). The effects of rhBMP-2 on pedicle screw pullout force and its potential to improve spinal fixation have not previously been investigated. We hypothesized that rhBMP-2 could stimulate bone growth in and around novel cannulated and fenestrated pedicle screws to improve early bone purchase. The objective of this study was to investigate the early term effectiveness of rhBMP-2 delivered to the lumbar pedicle screw sites to effect pedicle screw fixation in a sheep lumbar spine model without a bone graft for spine fusion. rhBMP-2 on an ACS carrier was delivered in and around specially designed cannulated/fenestrated pedicle screws. Two control groups (empty screw and ACS with buffer) were also evaluated. Biomechanical testing, undecalcified histology with microradiography, and quantitative histomorphometry were used to evaluate the holding power and bone formation within and adjacent to the novel pedicle screws at 6 and 12 weeks post-operatively.

## Methods

### *Animal model and study groups*

The sheep lumbar spine model has been specifically chosen because of the biomechanical similarities between the sheep and human lumbar spine (28,29). Under an IACUC approved study, eight skeletally mature female sheep underwent destabilizing laminectomies at L2–L3 and L4–L5 followed by stabilization with pedicle screw and rod constructs. No bone graft was placed in the intertransverse process space. All portions of this project involving animals were conducted in accordance with the policies, regulations, and standards set forth under the current USDA Animal Welfare Act and the current Public Health Service Policy using the Guide for the Care and Use of Laboratory Animals.

An ACS carrier was used to deliver 0.15 mg of rhBMP-2 (Medtronic, Memphis, TN, USA) at a dose concentration of 0.43 mg/cm$^3$ within and around specially designed 35 mm long 5.5 mm diameter cannulated and fenestrated titanium pedicle screws as seen in *Figure 1*. A volume of 0.1 cm$^3$ of rhBMP-2/ACS (0.043 mg of rhBMP-2) was placed in the cannulated and fenestrated screw and 0.25 cm$^3$ of rhBMP-2/ACS (0.107 mg of rhBMP-2) was placed around the threads of the screw. Three sets of three fenestrations (2-mm in diameter, 3-mm apart) were located 120 degrees apart around the cannula. The pedicle screw design was created to allow bone growth through the screw in order to improve mechanical interlocking between the pedicle screws and the newly formed bone of the vertebral body.

Two constructs with four pedicle screws at each of the L2–L3 and L4–L5 levels were created with a rod (5.5 mm diameter) connecting two pedicle screws without a cross link. As seen in *Table 1*, sheep functional spinal units (FSU's) were designated to one of four treatment groups. All four pedicle screws from the same FSU contained the same treatment. Randomization was performed so that for each vertebral body, one pedicle screw was analyzed by biomechanical testing, while the contralateral pedicle screw was analyzed by undecalcified histology and histomorphometry.

### *Biomechanical assessment*

At the time of testing, set screws and rods were removed with each FSU being separated into two vertebral bodies in the axial plane through the disc space. The biomechanical test

 

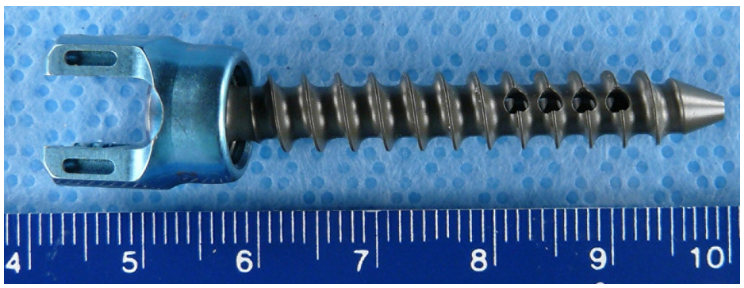


**Figure 1** This figure shows the cannulated and fenestrated pedicle screw used for all treatment groups during the study.

**Table 1** Table of treatment groups

| Group name | Time point (weeks) | Material placed in and around screw | Number of treated screws (N) in each group |
|---|---|---|---|
| 6-week Empty | 6 | Nothing | 16 |
| 6-week BMP | 6 | 0.15 mg of rhBMP-2 | 16 |
| 12-week ACS | 12 | ACS alone | 16 |
| 12-week BMP | 12 | 0.15 mg of rhBMP-2 | 16 |

rhBMP, recombinant human bone morphogenetic protein-2; ACS, absorbable collagen sponge.

was performed on one screw (randomly selected between the left and the right) at a time leaving the rest of the vertebral body intact with the contralateral screw designated for histology. Pullout tests were conducted using a servo hydraulic material testing machine (MTS model 809, MTS Corporation, Eden Prairie, MN, USA). A specially designed pullout jig was fitted to the set screw threading on the tulip portion of the screw head. Alignment of the screw during the biomechanical pullout test was facilitated using a guide pin placed within the cannulated aspect of the screw. Once the screw head and the pullout jig were aligned, the vertebral body was potted in dental cement, mounted to the MTS base, and the screw was pulled out at a constant displacement rate of 0.5 mm/sec until pullout occurred or the screw failed. Failure was defined as the point where a sharp decrease in the pullout force was detected. Three distinct biomechanical parameters were calculated from the force-displacement plot for each tested screw: the maximum pullout force, pullout stiffness from the linear region of the force-displacement curve, and the energy absorbed up to the failure point.

### *Undecalcified histology and microradiography*

Of the 32 pedicle screws designated for undecalcified histology, 16 were sectioned at a right angle to the long axis of the screw in the coronal plane (designated axial sections) and 16 were sectioned parallel to the long axis of the screw in the sagittal plane (designated longitudinal sections). This resulted in a sample size for histology of four screws for each treatment group for each sectioning orientation. Approximately 5–7 axial sections and approximately 3–5 longitudinal sections were made through the fenestrated and cannulated aspects of each of the pedicle screws. Undecalcified axial and longitudinal sections were stained with trichrome stain and then radiographed using a microradiography unit and spectroscopic film. Microradiographs were scanned using image analysis software (Image Pro Plus Software v 5.0, Media Cybernetics, Silver Spring, MD, USA) running on a Windows XP workstation. A video camera (Model DFC 280, Leica Microsystems, Cambridge, UK) was used to acquire black and white (8 bit gray scale) digital images of the microradiographs. Microradiographs were scanned and analyzed by quantitative histomorphometry as described below.

### *Quantitative histomorphometry*

Percent peri-implant bone: as seen in *Figure 2A*, on axial microradiograph images taken through the fenestrated areas of the screws, a fixed 7.5 mm diameter circular area of interest (AOI) was centered on the middle of the screw. As seen in *Figure 2B*, on longitudinal microradiograph images taken in the region of the fenestrated areas of the screws, a 14 mm by 7.5 mm rectangular AOI was centered along

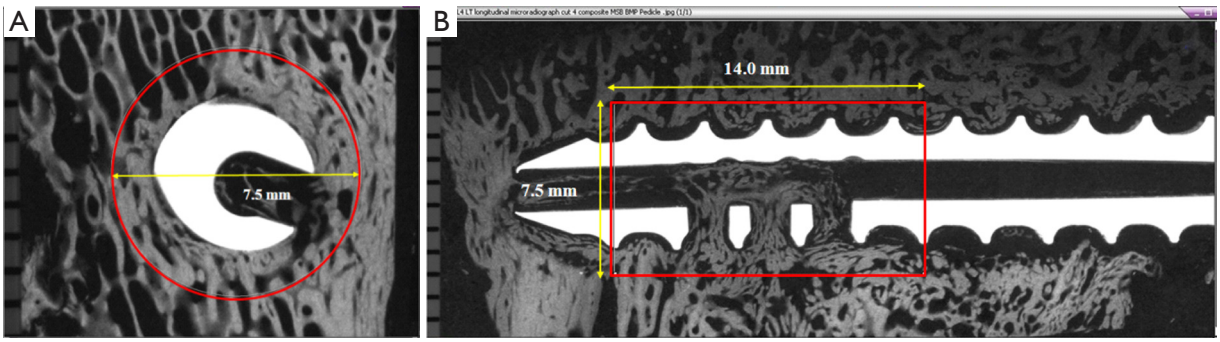


**Figure 2** These figures show the size and shape of the AOI used to measure bone quantity and quality in axial and longitudinal microradiographs. (A) Circular AOI used in axial microradiographs to measure the quantity and quality of peri-screw bone; (B) rectangular AOI used in longitudinal microradiographs to measure the quantity and quality of peri-screw bone. AOI, area of interest.

the length of the screw in the fenestrated region. These AOI's were used to determine the quantity and quality of bone adjacent to and within the fenestrated and cannulated aspects of the screw. Using image analysis, segmentation was selected and applied to the microradiograph image to determine the range of gray scales that corresponded to bone on the microradiograph. Images were segmented so that the least dense mineralized woven bone was assigned the lowest gray scale value and the most densely mineralized trabecular bone was assigned the highest gray scale value. This was determined on a case-by-case basis for the most accurate result. The pedicle screw and anything which was not bone was excluded from the measurements. With these gray scale ranges corresponding to bone being applied, a histogram for the region of interest was created and the percentage of bone (by area) in the circular/rectangular AOI was measured.

Peri-implant bone relative density: images were segmented so that the least dense mineralized woven bone was assigned the lowest gray scale value and the most densely mineralized trabecular bone was assigned the highest gray scale value. This was determined on a case-by-case basis for the most accurate result. The pedicle screw and anything which was not bone was excluded from the measurements. The bone inside the AOI described above was divided into four equal divisions based on the gray scale. Division 1 represented the lowest density of bone and Division 4 represented the highest density of bone. The percentage of bone in each quartile/division was measured on each microradiograph.

### *Data analysis*

Analysis of variance (ANOVA) was performed on the three parameters collected from the pullout test to study the effects of treatment. The same test was also performed on the histomorphometric variables including percent of bone in the area adjacent to the screw as well as percentage bone in each division of bone density. Whenever significant findings were obtained ($P<0.05$), further post-hoc Bonferroni/Dunn comparisons were conducted to identify groups with significant difference ($P<0.0083$). Linear correlation between the pullout variables and relative bone density of each pair of pedicle screws was performed to assess association between the two analyses.

## Results

### *Biomechanics results*

None of the cannulated fenestrated screws failed during the in-life portion of the study. Among the 32 screws for the pullout test, eight of the screws (four from the 6-week Empty group and four from the 12-week ACS group) failed at very high loads during the biomechanical test (before the screw could be completely pulled out of the bone). Failure occurred either (A) between the universal coupling joint of the screw and screw head or (B) through one of the fenestrated holes in the shaft of the screw. In the 6-week BMP group, four screws from one animal were removed from the analysis as outliers (defined as those data points with a deviation in value from the group mean by 2.5 times or more). The pullout force values of these screws, ranging from 121 to 425 N, was significantly lower than the group mean, and histologic evidence of infection was found at the site of their contralateral screws. Similarly, the two screws from another animal (one in the 12-week ACS group and one in the 12-week BMP group) were removed as outliers. The pullout force values for these two screws were

 

**Table 2** Results from pullout tests and statistical comparisons

| Pullout parameter | 6-week Empty | 6-week BMP | 12-week ACS | 12-week BMP |
|---|---|---|---|---|
| Force (N) | 3,720±932 †‡ | 2,070±908 | 3,190±728 | 2,330±550 |
| Stiffness (N/mm) | 1,570±414 | 1,060±201 | 1,740±529 | 1,510±78 |
| Energy (Nm) | 5.9±2.4 ‡ | 2.8±1.8 | 3.8±1.9 | 2.4±0.9 |

†, represents significantly higher value than the 6-week BMP group; ‡, represents significantly higher value than the 12-week BMP group. ACS, absorbable collagen sponge; BMP, bone morphogenetic protein.

151 and 141 N respectively. For all six outliers, peri-implant radiolucency was observed on axial radiographs. With these outliers removed, the number of specimens for biomechanical evaluation became n=4 for the 6-week BMP group, and n=7 for the 12-week ACS group and the 12-week BMP group.

The mean (± standard deviation) pullout force, stiffness, and energy at failure for the four study groups are presented in *Table 2*. The empty 6-week group demonstrated the highest mean pullout force at 3,720 N, while both BMP groups had a mean pullout force of approximately half that at 2,000 N. Bonferroni/Dunn tests showed that the 6-week Empty group had significantly higher pullout force than both the 6-week BMP group (P<0.0024) and the 12-week BMP group (P<0.0025). The mean pullout stiffness of the 12-week BMP group showed a significant trend of improved stiffness over the 6-week BMP group (P<0.034), while the highest stiffness was observed in the 12-week ACS group. The highest mean energy absorbed up to the failure point was observed in the 6-week Empty group. The 12-week BMP group showed the lowest required energy, despite the improved stiffness over the 6-week BMP group. The difference in energy absorbed up to the failure point between the 6-week Empty group and 12-week BMP group was statistically significant (P<0.001).

### *Undecalcified histology and microradiography*

In the 6-week Empty group, good bone contact was observed circumferentially along most of the outer diameter of the screw in the axial sections and along the length of the screw ventrally in the longitudinal sections. Bony trabeculae were found within fenestrations and the cannulated aspect of the screw with good bone contact ventrally in most samples. A sample microradiograph from the 6-week Empty group is seen in *Figure 3A*. In contrast, bone contact, on peri-implant interfaces or bone ingrowth within cannulation or fenestrations, was observed less frequently in the 6-week BMP group. As seen in a sample microradiograph from the 6-week BMP group in *Figure 3B*, extensive bone remodeling was observed around the screws, and microradiographs showed hypodense osteopenic trabeculae in these remodeled regions. Fluid- or blood-filled cysts were observed ventral to some of the screws in the 6-week BMP group.

In five of the six screws from the 12-week ACS group, good bone contact was observed circumferentially along the outer diameter of the screw in the axial sections and along the length of the screw ventrally and to a lesser degree dorsally in the longitudinal sections. Some bone growth was found within the fenestrated and cannulated aspects of the screws in the 12-week ACS group. Microradiographs showed isodense bone of normal trabecular thickness in peri-implant tissues. A sample microradiograph from the 12-week ACS group is seen in *Figure 3C*. Lack of bone contact at the screw interface was observed in many samples from the 12-week BMP group. The screws were often surrounded by thin to thick intervening fibrous tissues. Some bony trabeculae were observed within the fenestrated and cannulated aspects of the screw. A sample microradiograph from the 12-week BMP group is seen in *Figure 3D*. Fluid- or blood-filled cysts were observed ventral to some of the screws in the 12-week BMP group. A sample stained undecalcified section showing a blood filled cyst ventral to one of the screws in the 12-week BMP group is seen in *Figure 3E*. As seen in longitudinal microradiographs in *Figure 3A,B,C,D*, regardless of treatment group, the dorsal aspect of many screws showed a lack of bone contact even though the anterior aspect of the screws showed good bone contact.

### *Histomorphometric results*

Percent peri-implant bone: the mean (± standard deviation) percentages of bone in the circular or rectangular AOI adjacent to the screws from each group are presented in *Figure 4A,B*. In axial microradiographs, the highest percentage of bone by area was found in the 6-week Empty group (71.4%±3.1%), while the lowest was found in the 6-week BMP group (52.0%±18.1%). However, ANOVA showed no significant difference between the percentages of bone in any of the four

 

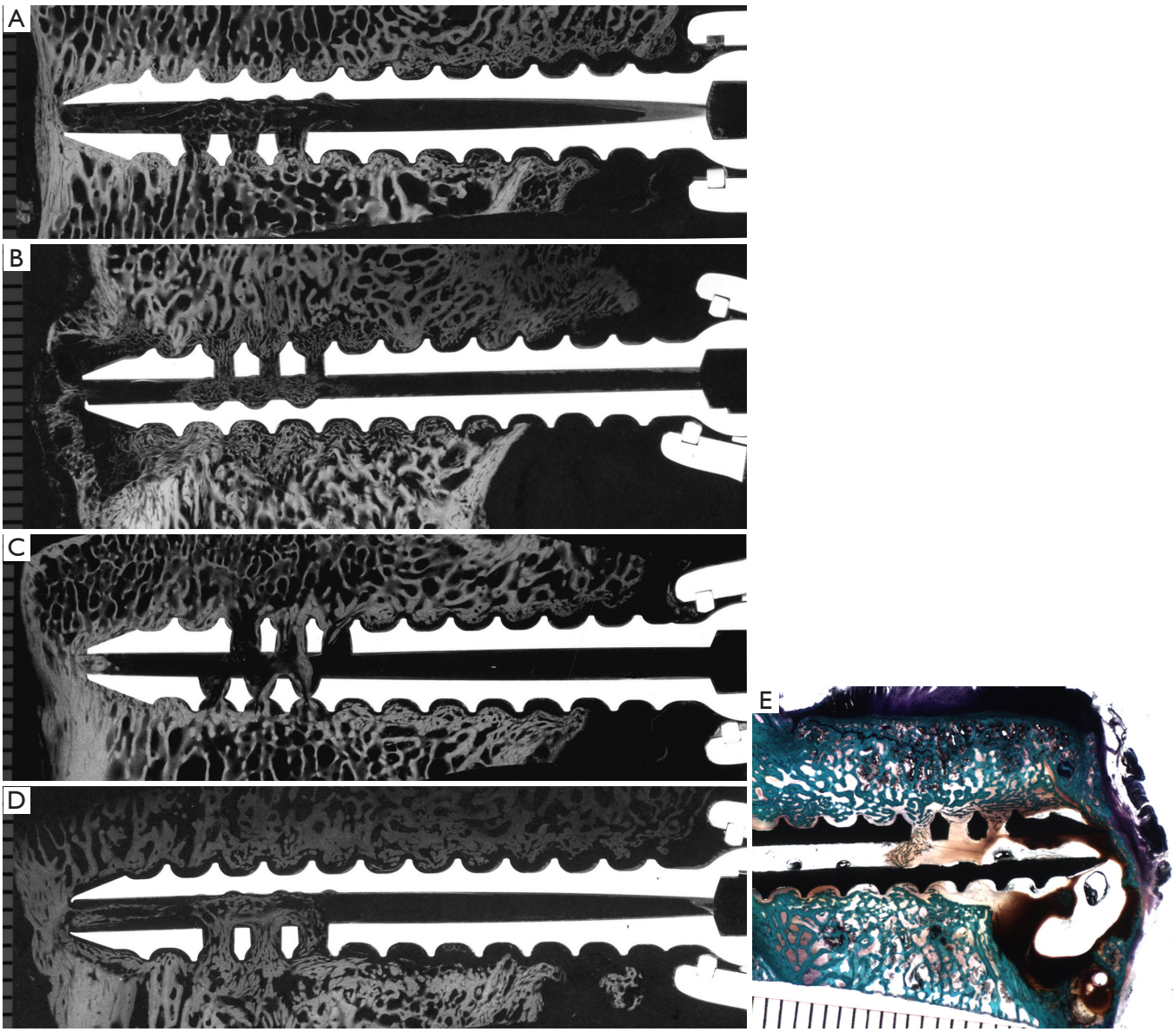


**Figure 3** These figures show representative longitudinal microradiographs from all treatment groups as well as a stained undecalcified section showing a blood-filled cyst. (A) Sample longitudinal microradiograph from the 6-week Empty group showing quantity and quality of peri-screw bone; (B) sample longitudinal microradiograph from the 6-week BMP group showing quantity and quality of peri-screw bone; (C) sample longitudinal microradiograph from the 12-week buffer ACS group showing quantity and quality of peri-screw bone; (D) sample longitudinal microradiograph from the 12-week BMP group showing quantity and quality of peri-screw bone; (E) sample stained undecalcified section showing a blood filled cyst ventral to one of the screws in the 12-week BMP group. (Trichrome stain, mm scale in field). ACS, absorbable collagen sponge; BMP, bone morphogenetic protein.

groups (P=0.24). Similar to the axial sections, although to a lesser extent, the highest percentage of bone in longitudinal microradiographs was found in the 6-week Empty group (57.4%±3.3%), while the lowest percentage of bone was found in the 6-week BMP group (37.2%±14.7%). ANOVA revealed a marginal level of significance (P=0.06) among the four groups, and post-hoc tests showed that the 6-week Empty group had marginally higher percentage of bone than both the 6- and 12-week BMP groups.

Peri-implant bone density: *Figure 5A,B,C,D* show

 

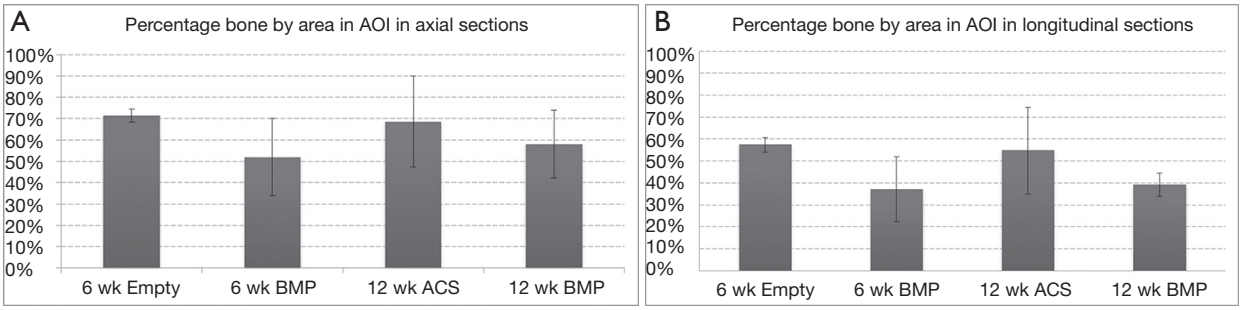


**Figure 4** These figures show the mean (± standard deviation) of the percentage of bone in the AOI for all four treatment groups. (A) Graph showing the percentage of bone in circular AOIs for axial microradiographs for all four treatment groups; (B) graph showing the percentage of bone in rectangular AOIs for longitudinal microradiographs for all four treatment groups. AOI, area of interest. wk, week.

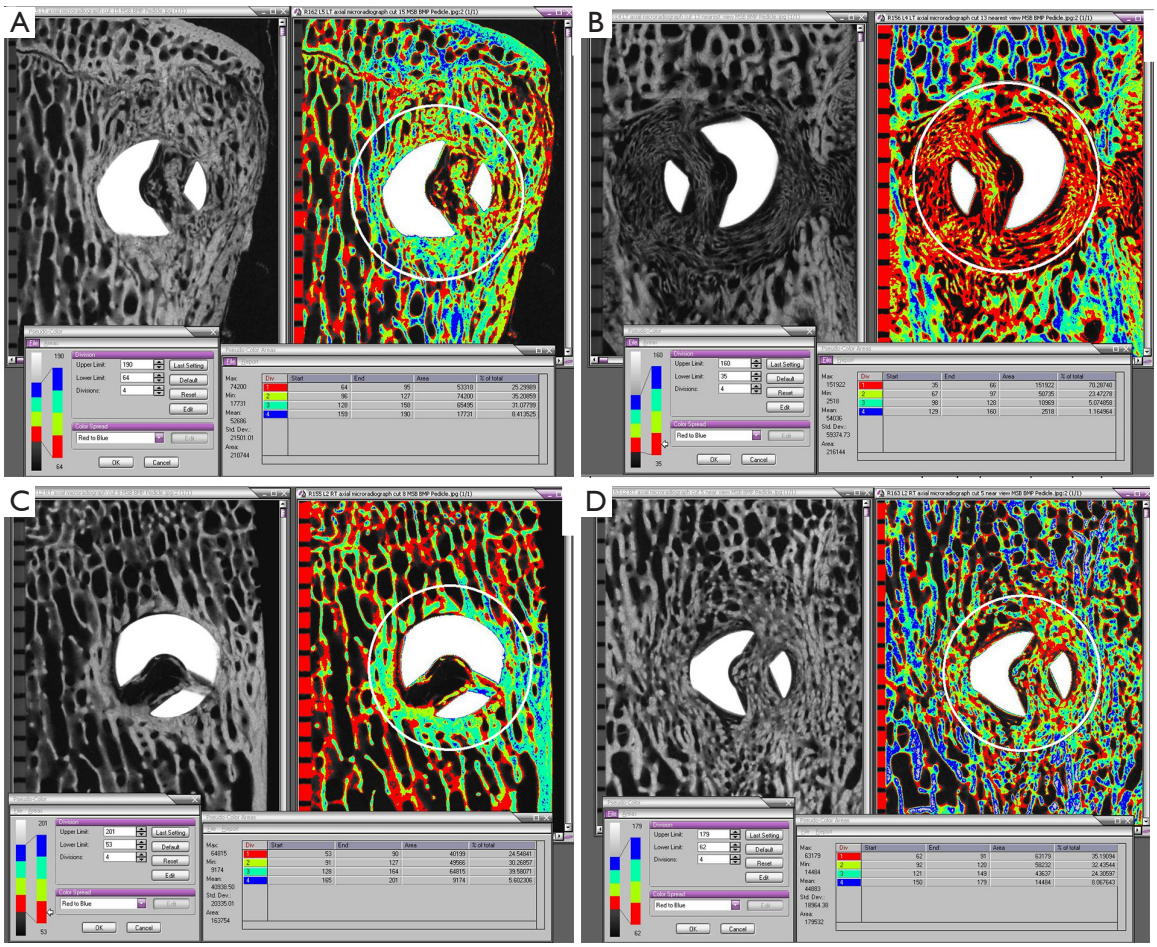


**Figure 5** These figures show representative axial microradiographs and the corresponding quantitative histomorphometry images and results for all four treatment groups. (A) Sample axial microradiograph and corresponding histomorphometry image from the 6-week Empty group showing quantity and quality of peri-screw bone; (B) sample axial microradiograph and corresponding histomorphometry image from the 6-week BMP group showing quantity and quality of peri-screw bone; (C) sample axial microradiograph and corresponding histomorphometry image from the 12-week buffer ACS group showing quantity and quality of peri-screw bone; (D) sample axial microradiograph and corresponding histomorphometry image from the 12-week BMP group showing quantity and quality of peri-screw bone. ACS, absorbable collagen sponge; BMP, bone morphogenetic protein.

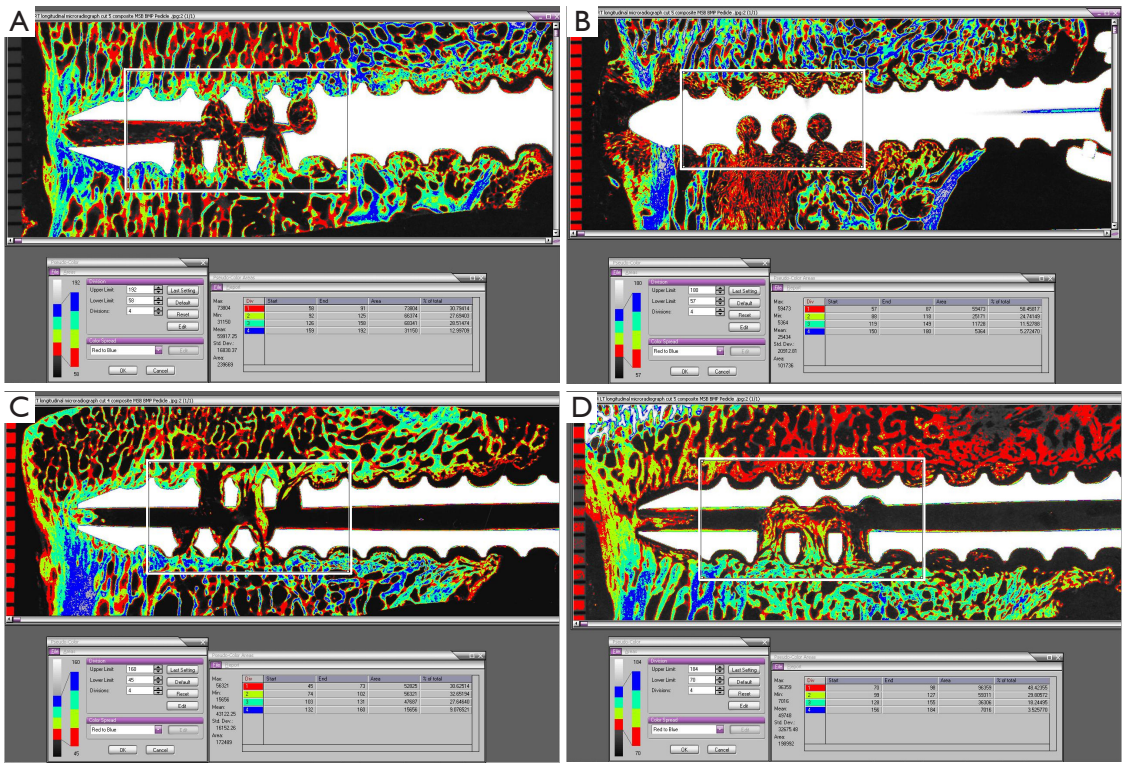


**Figure 6** These figures show representative longitudinal microradiographs and the corresponding quantitative histomorphometry images and results for all four treatment groups. (A) Sample longitudinal histomorphometry image from the 6-week Empty group showing quantity and quality of peri-screw bone; (B) sample longitudinal histomorphometry image from the 6-week BMP group showing quantity and quality of peri-screw bone; (C) sample longitudinal histomorphometry image from the 12-week buffer ACS group showing quantity and quality of peri-screw bone; (D) sample longitudinal histomorphometry image from the 12-week BMP group showing quantity and quality of peri-screw bone. ACS, absorbable collagen sponge; BMP, bone morphogenetic protein.

representative microradiographs and corresponding quantitative histomorphometry images with bone density quartiles for axial sections through the screws for all of the treatment groups. *Figure 6A,B,C,D* show representative quantitative histomorphometry images with bone density quartiles for longitudinal sections through the screws for all of the treatment groups. The mean (± standard deviation) percentage of bone in each of the four density divisions for both axial and longitudinal sections is plotted in *Figure 7A,B*. The distribution plot shows that all four groups had less than 10% of the adjacent bone from the highest density division (Division 4), and approximately 30% of the adjacent bone from the lower middle density division (Division 2). The groups varied significantly in the percentage of bone in the weakest density division (Division 1) and the upper middle density division (Division 3). The 6-week BMP group had the highest percentage bone area from Division 1 (45.5%) which was significantly higher than the other three groups (P<0.001, Bonferroni/Dunn). The 6-week BMP group also had the lowest percentage bone from Division 3 (16.1%), which was significantly lower than the other three groups (P<0.0005, Bonferroni/Dunn).

Similar to the results from the axial sections, the distribution plot (*Figure 7B*) for the longitudinal sections shows that all four groups had less than 10% of the adjacent bone from the highest density division (Division 4), and approximately 30% of the adjacent bone from the lower middle density division (Division 2). The groups varied significantly in the weakest density division (Division 1) and the upper middle density division (Division 3). The 6-week BMP group had the highest percentage of bone from Division 1 (49.6%), and was significantly higher than the 12-week ACS group (26.3%, P<0.0001, Bonferroni/Dunn) and 6-week Empty group (34.7%, P<0.002). The 6-week BMP group also had the lowest percentage of bone from

 

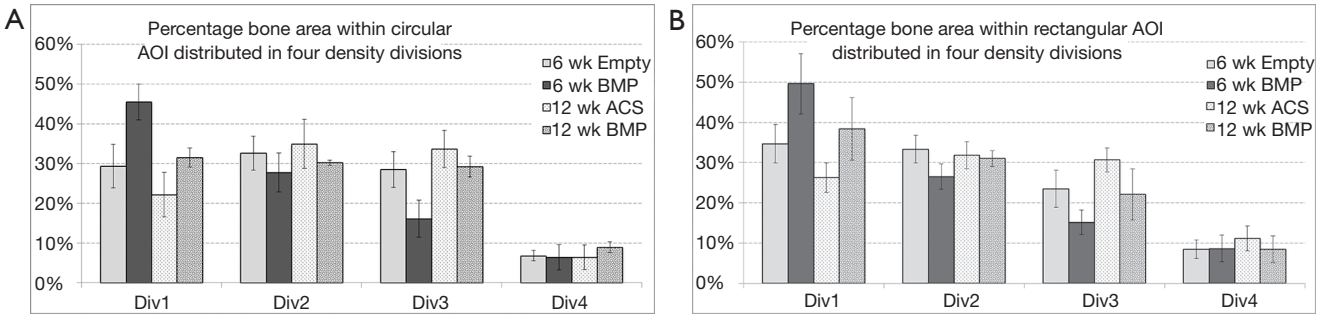


**Figure 7** These figures show mean (± standard deviation) of the percentage of bone in each of the four density divisions within the AOI for axial and longitudinal sections. (A) The mean (± standard deviation) percentage of bone in each of the four density divisions for axial sections for the four treatment groups is plotted; (B) the mean (± standard deviation) percentage of bone in each of the four density divisions for longitudinal sections for the four treatment groups is plotted. ACS, absorbable collagen sponge; BMP, bone morphogenetic protein, wk, week.

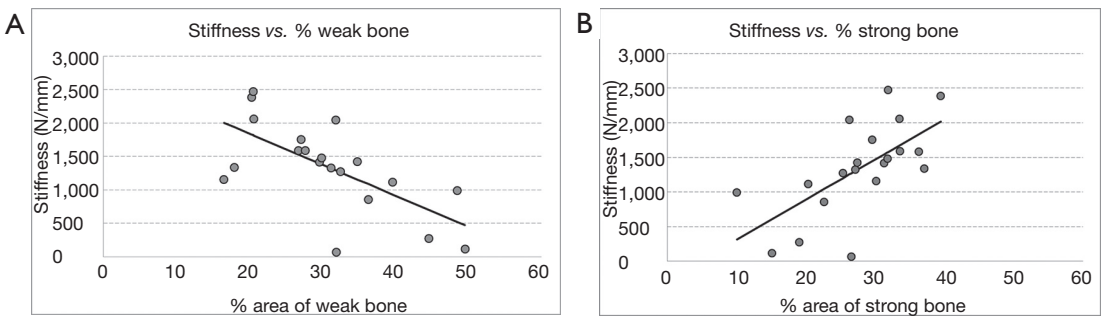


**Figure 8** These figures show scatter plots with the correlation between the pullout stiffness and percentage area of least dense (or dense) bone in circular AOI in axial sections. (A) Scatter plot showing the reverse correlation between the percentage area of Division 1 (least dense bone) in the circular AOI in an axial section and the pullout stiffness from the biomechanical test (R=0.66, P<0.001); (B) scatter plot showing correlation between the percentage of bone in Division 3 (dense bone) in the circular AOI in axial sections and the pullout stiffness from the biomechanical test (R=0.65, P<0.002). AOI, area of interest.

Division 3 (15.2%), and was significantly lower than the 12-week ACS group (30.7%, P<0.0003).

Correlation between pullout variables and histomorphometry density: when pullout force and stiffness data were paired with the measured percentages of bone in bone density quartiles for each pair of pedicle screws on the same vertebral body (same treatment), a statistically significant but moderate correlation was found between quantitative histomorphometric findings of hypodense trabeculae with the low biomechanical pullout variables. *Figure 8A* shows the reverse correlation between the percentage area of Division 1 (least dense bone) in the circular AOI in an axial section and the pullout stiffness from the biomechanical test (R=0.66, P<0.001). A similar trend of correlation was shown between the pullout strength from the biomechanical test and the percentage of bone in Division 1 (R=0.58, P<0.007).

Similarly, a correlation was found between quantitative histological findings of dense trabeculae with the high biomechanical pullout variables. *Figure 8B* shows the correlation between the percentage of bone in Division 3 (dense bone) in the circular AOI in axial sections and the pullout stiffness from the biomechanical test (R=0.65, P<0.002). Additionally, the correlation between the percentage of bone in Division 3 and the pullout strength was also significant (R=0.48, P<0.03).

## Discussion

rhBMP-2 was unable to improve bony purchase of the cannulated and fenestrated pedicle screws compared to both control groups. The pullout force values measured in our control groups [3,720 N (6-week Empty) and 3,190 N

(12-week ACS)] with the cannulated and fenestrated pedicle screws were higher than the 2,200 N previously reported by Sandén *et al.* with unmodified screws in the sheep cohort where no radiolucencies were detected at the screw-bone interface (30). In our study, both rhBMP-2 groups with cannulated and fenestrated pedicle screws had pullout force values exceeding 2,000 N which was comparable to the Sanden study results (30). We suspect that the fenestrated and cannulated design of the screws as well as bicortical purchase of screws that were placed laterally in the smaller sheep vertebral bodies may be factors for the higher holding power.

Four screws in each control group failed during biomechanical testing, which is rarely found in the literature. None of the cannulated fenestrated screws failed during the in-life portion of the study. Clinically, it is unlikely that the screws would experience such a high pullout force to cause fracture *in vivo*. We suggest that the high pullout force is likely related to the cannulated and fenestrated design of the pedicle screws, which allows for bone growth through the fenestrations and within the cannulated aspect of the screw, not just bone between threaded regions associated with a traditional pedicle screw design.

Results from our study are consistent with the findings from Sandén *et al.* indicating that the presence or absence of peri-screw radiolucency has a significant influence on the pullout force (30). In Sanden's series of pedicle screws with peri-implant radiolucencies, the mean pullout force was 243 N (30). This was consistent with our pullout force data which ranged from 121 to 425 N for our six "outliers" where peri-screw radiolucencies were observed. Histological assessment further confirmed poor bone contact in all of these cases.

Bone quality and not quantity was correlated with biomechanical parameters measured in the current study. Statistical analysis of the quantitative histomorphometry data showed that the amount of bone formed in and around the pedicle screws was comparable between all four treatment groups. Qualitatively, rhBMP-2 induced bone in and around the screws was observed to be hypodense and osteopenic, especially at the relatively short 6 week post-operative time point studied. Quantitative histomorphometry on microradiographs from both longitudinal and axial sections showed that rhBMP-2 induced bone had statistically significant lower density bone compared to the control group at 6 weeks. Biomechanical variables from the pullout test showed moderate but significant correlations with the relative density obtained from quantitative histomorphometric analysis. Thus, it would appear that rhBMP-2 placed in and around the screws in the current study caused peri-screw bone remodeling resulting in early hypodense trabeculae that provided less resistance to pullout forces in comparison to control groups.

Bone remodeling adjacent to rhBMP-2 treated screws was noted in this study. In a safety profile regarding the use of BMP's in the spine, Poynton and Lane have indicated that bone resorption occurs before bone formation with BMP's (31). Transient bone resorption as well as seromas and hematomas associated with rhBMP-2 in corticocancellous bony defects have been documented in sheep (32). Seeherman *et al.* investigated the chronologic sequence of transient bone resorption and formation associated with rhBMP-2/ACS in cancellous bone in nonhuman primate femoral core metaphyseal defects at a concentration of 1.5 mg/mL (33). Their results showed that bone resorption at 1 to 2 weeks precedes bone formation following the administration of rhBMP-2 delivered in an ACS in metaphyseal bone, although bone resorption was limited when a calcium phosphate carrier was used instead of ACS (33,34). It is possible that the dose of rhBMP-2 used in the current study was too high as a minimum effective dose is not known in the sheep model. It is known that release kinetics of rhBMP-2 on ACS is high, which could lead to increased resorption (35). In a sheep lumbar interbody fusion model, Bae *et al.* found that transient bone resorption areas associated with rhBMP-2 were fully healed by 12 weeks. In the current sheep lumbar pedicle screw model, transient bone resorption areas were not fully healed by 12 weeks (36). Different BMP carriers or a different delivery method might stimulate less peri-implant bone remodeling in this model. If the use of rhBMP-2 with pedicle screws is to be successfully translated clinically, delivery of rhBMP-2 should be carefully controlled to prevent excessive bone remodeling which could cause early screw loosening and subsequent failure of the spinal construct.

## Acknowledgements

Institutional Research support for this study was provided by Medtronic Spinal and Biologics. The authors wish to thank and acknowledge Sharath Chandra Venkata Chedella, BDS, MS for technical expertise in histologic processing of the tissues as well as Linda McGrady, MS, for technical expertise in biomechanical testing. The Medical College

 

of Wisconsin received research funding paid directly to the institution from Medtronic Spinal and Biologics in support of the study.

## Footnote

*Conflicts of Interest:* The Medical College of Wisconsin received research funding paid directly to the institutions from Medtronic Spinal and Biologics in support of the study. The sponsor/funding source had no involvement in the collection, analysis and interpretation of data or in the writing of the report or in the decision to submit the article for publication. JM Toth and CK Patel serve as scientific consultants to Medtronic.

*Ethical Statement:* The Institutional Animal Care and Use Committee of Thomas D. Morris, Inc. approved this protocol (#08-003).

## References

1. Ames CP, Acosta FL Jr, Chi J, et al. Biomechanical comparison of posterior lumbar interbody fusion and transforaminal lumbar interbody fusion performed at 1 and 2 levels. Spine (Phila Pa 1976) 2005;30:E562-6.
2. Best NM, Sasso RC. Efficacy of translaminar facet screw fixation in circumferential interbody fusions as compared to pedicle screw fixation. J Spinal Disord Tech 2006;19:98-103.
3. Eskander M, Brooks D, Ordway N, et al. Analysis of pedicle and translaminar facet fixation in a multisegment interbody fusion model. Spine (Phila Pa 1976) 2007;32:E230-5.
4. Lee SS, Lenke LG, Kuklo TR, et al. Comparison of Scheuermann kyphosis correction by posterior-only thoracic pedicle screw fixation versus combined anterior/posterior fusion. Spine (Phila Pa 1976) 2006;31:2316-21.
5. Weinstein JN, Rydevik BL, Rauschning W. Anatomic and technical considerations of pedicle screw fixation. Clin Orthop Relat Res 1992;284:34-46.
6. Cook SD, Salkeld SL, Whitecloud TS 3rd, et al. Biomechanical evaluation and preliminary clinical experience with an expansive pedicle screw design. J Spinal Disord 2000;13:230-6.
7. Krenn MH, Piotrowski WP, Penzkofer R, et al. Influence of thread design on pedicle screw fixation. Laboratory investigation. J Neurosurg Spine 2008;9:90-5.
8. Lill CA, Schneider E, Goldhahn J, et al. Mechanical performance of cylindrical and dual core pedicle screws in calf and human vertebrae. Arch Orthop Trauma Surg 2006;126:686-94.
9. Burval DJ, McLain RF, Milks R, et al. Primary pedicle screw augmentation in osteoporotic lumbar vertebrae: biomechanical analysis of pedicle fixation strength. Spine (Phila Pa 1976) 2007;32:1077-83.
10. Chang MC, Liu CL, Chen TH. Polymethylmethacrylate augmentation of pedicle screw for osteoporotic spinal surgery: a novel technique. Spine (Phila Pa 1976) 2008;33:E317-24.
11. Chen LH, Tai CL, Lai PL, et al. Pullout strength for cannulated pedicle screws with bone cement augmentation in severely osteoporotic bone: influences of radial hole and pilot hole tapping. Clin Biomech (Bristol, Avon) 2009;24:613-8.
12. Frankel BM, D'Agostino S, Wang C. A biomechanical cadaveric analysis of polymethylmethacrylate-augmented pedicle screw fixation. J Neurosurg Spine 2007;7:47-53.
13. Yi X, Wang Y, Lu H, et al. Augmentation of pedicle screw fixation strength using an injectable calcium sulfate cement: an in vivo study. Spine 2008;33:2503-9.
14. Masaki T, Sasao Y, Miura T, et al. An experimental study on initial fixation strength in transpedicular screwing augmented with calcium phosphate cement. Spine 2009;34:E724-8.
15. Hashemi A, Bednar D, Ziada S. Pullout strength of pedicle screws augmented with particulate calcium phosphate: an experimental study. Spine J 2009;9:404-10.
16. Taniwaki Y, Takemasa R, Tani T, et al. Enhancement of pedicle screw stability using calcium phosphate cement in osteoporotic vertebrae: in vivo biomechanical study. J Orthop Sci 2003;8:408-14.
17. Milcan A, Ayan I, Zeren A, et al. Evaluation of cyanoacrylate augmentation of transpedicular screw pullout strength. J Spinal Disord Tech 2005;18:511-4.
18. Fini M, Giavaresi G, Greggi T, et al. Biological assessment of the bone-screw interface after insertion of uncoated and hydroxyapatite-coated pedicular screws in the osteopenic sheep. J Biomed Mater Res A 2003;66:176-83.
19. Hasegawa T, Inufusa A, Imai Y, et al. Hydroxyapatite-coating of pedicle screws improves resistance against pull-out force in the osteoporotic canine lumbar spine model: a pilot study. Spine J 2005;5:239-43.
20. Sandén B, Olerud C, Larsson S. Hydroxyapatite coating enhances fixation of loaded pedicle screws: a mechanical in vivo study in sheep. Eur Spine J 2001;10:334-9.
21. Upasani VV, Farnsworth CL, Tomlinson T, et al. Pedicle

 

screw surface coatings improve fixation in nonfusion spinal constructs. Spine 2009;34:335-43.
22. McKay B, Sandhu HS. Use of recombinant human bone morphogenetic protein-2 in spinal fusion applications. Spine 2002;27:S66-85.
23. Sandhu HS, Toth JM, Diwan AD, et al. Histologic evaluation of the efficacy of rhBMP-2 compared with autograft bone in sheep spinal anterior interbody fusion. Spine 2002;27:567-75.
24. Valentin-Opran A, Wozney J, Csimma C, et al. Clinical evaluation of recombinant human bone morphogenetic protein-2. Clin Orthop Relat Res 2002;395:110-20.
25. Seeherman H, Wozney J, Li R. Bone morphogenetic protein delivery systems. Spine 2002;27:S16-23.
26. Boden SD, Zdeblick TA, Sandhu HS, et al. The use of rhBMP-2 in interbody fusion cages. Definitive evidence of osteoinduction in humans: a preliminary report. Spine 2000;25:376-81.
27. Burkus JK, Gornet MF, Dickman CA, et al. Anterior lumbar interbody fusion using rhBMP-2 with tapered interbody cages. J Spinal Disord Tech 2002;15:337-49.
28. Wilke HJ, Kettler A, Claes LE. Are sheep spines a valid biomechanical model for human spines? Spine 1997;22:2365-74.
29. Easley NE, Wang M, McGrady LM, et al. Biomechanical and radiographic evaluation of an ovine model for the human lumbar spine. Proc Inst Mech Eng H 2008;222:915-22.
30. Sandén B, Olerud C, Petren-Mallmin M, et al. The significance of radiolucent zones surrounding pedicle screws. Definition of screw loosening in spinal instrumentation. J Bone Joint Surg Br 2004;86:457-61.
31. Poynton AR, Lane JM. Safety profile for the clinical use of bone morphogenetic proteins in the spine. Spine 2002;27:S40-8.
32. Toth JM, Boden SD, Burkus JK, et al. Short-term osteoclastic activity induced by locally high concentrations of recombinant human bone morphogenetic protein-2 in a cancellous bone environment. Spine 2009;34:539-50.
33. Seeherman HJ, Li XJ, Bouxsein ML, et al. rhBMP-2 induces transient bone resorption followed by bone formation in a nonhuman primate core-defect model. J Bone Joint Surg Am 2010;92:411-26.
34. Seeherman HJ, Li XJ, Smith E, et al. rhBMP-2/calcium phosphate matrix induces bone formation while limiting transient bone resorption in a nonhuman primate core defect model. J Bone Joint Surg Am 2012;94:1765-76.
35. Geiger M, Lib RH, Friess W. Collagen sponges for bone regeneration with rhBMP-2. Adv Drug Deliv Rev 2003;55:1613-29.
36. Bae HW, Patel VV, Sardar ZM, et al. Transient Local Bone Remodeling Effects of rhBMP-2 in an Ovine Interbody Spine Fusion Model. J Bone Joint Surg Am 2016;98:2061-70.

**Cite this article as:** Toth JM, Wang M, Patel CK, Arora A. Early term effects of rhBMP-2 on pedicle screw fixation in a sheep model: histomorphometric and biomechanical analyses. J Spine Surg 2018;4(3):534-545. doi: 10.21037/jss.2018.06.19

 